J Mater Sci (2009) 44:3466–3471
DOI 10.1007/s10853-009-3462-3

ZrO_2 foams for porous radiant burners

Sergio Yesid Gómez · J. A. Escobar · O. A. Alvarez · C. R. Rambo · A. P. Novaes de Oliveira · D. Hotza

Received: 17 September 2008 / Accepted: 3 April 2009 / Published online: 20 April 2009

Abstract In this work, Y_2O_3-stabilized ZrO_2 (YSZ) foams with low relative density were developed through the replication method, for application as porous radiant burners. The ceramic foams were produced by impregnation of open-cell polyurethane foams with aqueous suspensions and different fractions of raw materials: ZrO_2–8% Y_2O_3 (8YSZ) powder, and additives. The materials were milled for 10–40 min. The impregnated foams were dried and submitted to a heat treatment for polyurethane elimination at 1000 °C for 1 h, with subsequent sintering of the remaining ceramic structure at 1600 °C for 2 h, which resulted in YSZ foams with low relative density (0.07). The structural analysis revealed a cellular structure with an average mechanical strength of 95.6 kPa. The radiation efficiency (>19%) was obtained by tests with different air/fuel ratio. The ceramic matrixes exhibited high performance and structural integrity at high operation temperatures (1400 °C).

S. Y. Gómez (✉) · J. A. Escobar · O. A. Alvarez
Group of Materials and Manufacture (CIPP-CIPEM), Department of Mechanical Engineering, University of Los Andes, Cra 1 Este No. 19A-40, Bogota, Colombia
e-mail: ser-gome@uniandes.edu.co

S. Y. Gómez · O. A. Alvarez
Design of Products and Processes Group (GDPP), Department of Chemical Engineering, University of los Andes, Cra 1 Este No. 19A-40, Bogota, Colombia

C. R. Rambo · A. P. N. de Oliveira · D. Hotza
Group of Ceramic and Glass Materials (CERMAT), Departments of Chemical and Mechanical Engineering (EQA/EMC), Federal University of Santa Catarina—UFSC, P.O. Box 476, Florianópolis, SC 88040-900, Brazil

Introduction

Nowadays the majority of the combustion process is conducted in free-flame burners, which exhibit relatively low thermal efficiencies [1]. In order to enhance combustion efficiency, different strategies have been used: recirculation of combustion gases, internal recirculation regions, combustion by stages, and the direct heating of the combustion zone through heat exchange with a porous solid matrix [2].

Studies in the field of combustion in porous media emerged at the beginning of the twentieth century with the design of the first boilers and muffle heaters [3] and the construction of radiant heat rooms, high temperature furnaces and kitchen stoves operated with natural gas [4]. Since its inception the combustion process in porous media has been widely investigated, several authors reported on its benefits, characterization, and improvement [3–6].

Combustion in porous media offers advantages over conventional burners; namely higher burner speed, higher flame stability with lesser noise emissions, lower temperatures in the combustion zone, rational use of fuel, as well as lower emissions of NO_x and CO [5]. Adoption of this technology contributes to considerable energy savings and environmental protection.

The improvement of combustion in porous media, has been driven forward by experimentation, modeling, and numerical simulation [6], together with the development of porous materials with high temperature and thermal shock resistances [7]. Ceramic foams can be manufactured by different methods, such as replication or polymeric sponge method, direct foaming, and foaming agents. The replication method, patented in 1963 by Schwartzwalder and Somers [8], is relatively simple and economical. It consists of the impregnation of a polymeric foam with slurries containing the appropriate additives, followed by a heat

treatment, a stage in which the additives are removed and the degradation of the polymeric sponge occurs, subsequently sintering the remaining ceramic structure [9].

This article reports on the manufacturing and characterization of porous ZrO_2–8% Y_2O_3 (YSZ) ceramic burners with low relative density. Rheological parameters were evaluated in order to optimize the replication method that was used to produce the ceramic foams.

Materials and methods

Materials

Aqueous ceramic suspensions were prepared with the following raw materials: (a) *Ceramic precursor*: zirconia powder stabilized with yttria (8YSZ, 8 mol% $D_{50} = 0.6$ μm (TZ-8YS, Tosoh, Japan); (b) *Dispersants*: ammonium poly-methacrylate (Darvan C, USA) and sodium silicate ($(Na_2O_3(SiO_2)_n$, $2 < n < 4$, Merck, Brazil); (c) *Binder*: polyvinyl acrylic (PVA, VETEC, Brazil). The description of the composition of each suspension system is shown in Table 1.

Processing

The materials of each suspension were weighed on a precision scale (Digimed KN500). The raw materials were mixed and ground in a planetary grinder (CT 242 Servitech, Brazil) with alumina balls (400 g in a 500 mL container) at 1720 rpm for 5 min without a dispersant. Then the dispersant was added and was ground for an additional (10–40 min).

Polyurethane foams (PUF) of 10 and 20 pores per inch (ppi) (FoamPartner GmbH, Switzerland) with dimensions 25 × 25 × 25 ± 1 mm were submerged in the suspension while they were simultaneously compressed to fill all the pores. Afterwards, the foams were subjected to manual compression to remove the excess of slurry and to promote an open cell structure. The samples were dried at room temperature for a period of 24 h. Subsequently the impregnated foams were subjected to a heat treatment in an electric furnace (Linn KK 260, Germany), to extract the support material and additives as well as pre-sintering the remaining ceramic structure at a temperature of 1000 °C for 1 h in air. The green ceramic foams were subsequently sintered at 1600 °C for 2 h in air.

Table 1 Composition and grinding time of the ceramic suspensions of YSZ, carried out in the experimental procedure

System	YSZ	Binder	Dispersant	Grinding time (min)
1	60 wt%	PVA 0.25 wt%	Na_2SiO_3 1 wt%	10
2				20
3				30
4				40
5	70 wt%			20
6				40
7		PVA 0.5 wt%	Darvan C 1 wt%	20
8				40
9				20
10	80 wt%			20

Characterization

Rheological measurements of the ceramic precursor suspensions were carried out with a viscometer of concentric cylinders (Thermo Haake, Model DC10, Germany). The thixotropy was measured by plotting the hysteresis curves of the rheograms and by calculating the values of the areas between the curves.

Polyurethane foams (PUF) with dimensions of 100 × 100 × 45 ± 1 mm and samples of ceramic foams with dimensions of 21 × 21 × 21 ± 3 mm (with different ppi) were used for compression strength tests. The tests were conducted at room temperature, using a universal testing machine (Instron, Model 4202, Canton, MA, USA), where the speed of the cross-head was set at 1 mm/min.

The morphology of polyurethane foams was analyzed by stereoscopy (Stereoscopy, Olympus-SZ60, Japan). The microstructural analysis of the foams was performed by scanning electron microscopy (SEM) (Philips, Model XL-30, Eindhoven, Netherlands). Total porosity, ε, of each sample was estimated by calculating the relationship between the geometric density and the real density according to the equation: $\varepsilon_v = (1 - \rho^*/\rho s)$. The anisotropy and ppi of the YSZ foams were obtained by analysis of photographs with 4× of optic zoom.

Tests in the porous burner were conducted with 8YSZ foams with 20 ppi and dimensions of 35 × 25 ± 0.1 mm (radius and height, respectively), in a test bank developed by Pereira [10], using methane as fuel. The burner was isolated with a refractory blanket (Durablanket 1400, Fiberfrax, UNIFRAX, USA). The temperatures were measured by four thermocouples (Omega, type R, Pt/Pt–13%Rh), 0.01 in, 50–1768 °C) with an accuracy of 0.25%.

Results and discussion

Figure 1 shows the stereographs of the polyurethane foams PUF with different ppi, containing the contoured geometrical features. Table 2 shows the results of the morphometric characterization of the PUF, obtained from the data

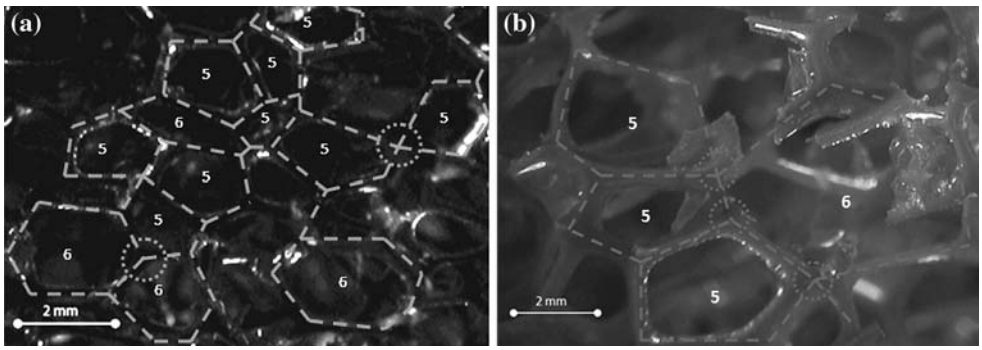

Fig. 1 Stereographs of the PUF foams: **a** 20 ppi; **b** 10 ppi

Table 2 Morphometric characterization of the PUF

Parameter	Symbol	PUF (10ppi)	PUF (20ppi)
Plateau stress (kPa)	σp	18	24
Densification deformation (mm/mm)	δd	0.7	0.8
Edge connectivity	Z_e	4	4
Face connectivity	Z_f	3	3
Mean value of edges per cell	n	5.14	5.14
Mean value of faces per cell	f	14	14
Porosity	ε_v	0.97	0.98

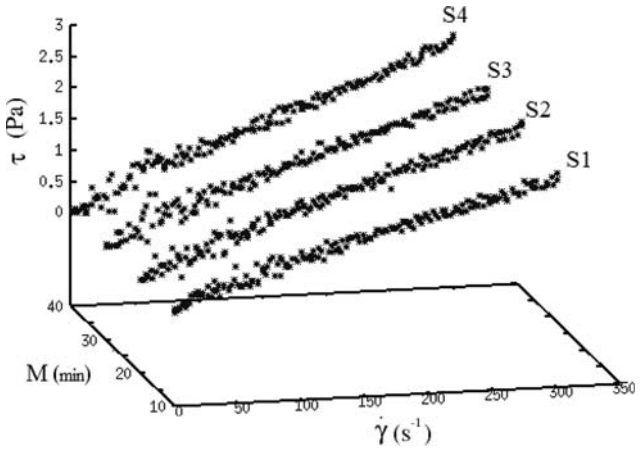

Fig. 2 Shear stress (τ) versus shear rate (γ) for the ceramic suspensions S1–S4. At different milling/grinding times (M)

of the stereographs in the Fig. 1. The impregnated samples were subjected to a constant (plateau) stress (σd) at a deformation of $\delta = 50\%$ in order to avoid the removal of larger amounts of suspension of the PUF. The morphometric parameters: edge connectivity (Z_e), face connectivity (Z_f), mean value of edges per cell (n) and the mean value of faces per cell (f); revealed an interconnected structure of open cells [11]. The PUF structures exhibit a high porosity ($\varepsilon_v \approx 0.98$) that is related the porosity in the YSZ foams.

Figure 2 shows the shear stress versus shear rate for the suspensions S1–S4 after different grinding times. The shear rate and the viscosity increased with the increasing of the solid fraction in suspension. For higher solid contents, the particles start to pack and the thickness of the hydrated inter-particle layers was reduced, decreasing the spaces between particles and promoting less sliding between them. Particles of a smaller size were obtained with a longer grinding time, which resulted in higher packing configuration in the suspension. A similar effect was described previously with the increase in the solid content (S1–S4). It was also observed that the quantity and binder type affects the thixotropy of the suspensions.

Figure 3 shows the shear stress versus shear rate for the suspensions S5–S10. Dispersant Darvan C favors thixotropy, compared with Na_2SiO_3. This was evidenced in systems with equal formulation conditions and grinding time S5 (Fig. 3a) and S9 (Fig. 3b). The effect of thixotropy and pseudoplasticity are desirable, because they are indicators of the suspension stability and also support impregnation [12]. Higher binder (PVA) amount promotes an increase in thixotropy (systems S6 and S8. Figure 3) and a higher initial viscosity in the system by forming a particulate structure. This structure breaks when subjected to a shear stress, leading to a less hindered movement and, therefore, to a lower viscosity. The rupture and the arrangement of the particles of the system promote differences in the hysteresis curves. The thixotropic systems are favorable for the impregnation process due to their high viscosity in steady state, which reduces the tendency of the particles toward sedimentation, avoiding solid–liquid separation. On the other hand, during flow conditions in these systems the viscosity decreases, facilitating the flow [13].

The suspension systems (S1–S4) were partially fixed in the polymeric structure. The low viscosity of these systems and the low affinity of polyurethane to wetness prevented the formation of the ceramic structures. The ceramic structures of the systems S1–S5 and S8 were broken in the first thermal cycle, due to the release of the support material in gas form and the temperature gradients generated in the structure. The thixotropic suspensions impregnated the PUF in a more adequate way (open cells,

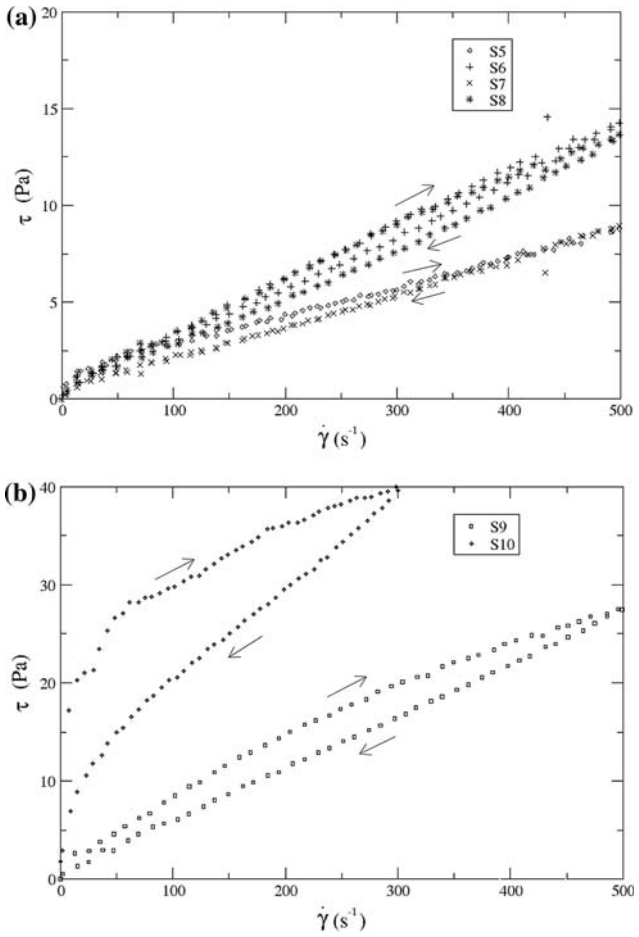

Fig. 3 Shear stress (τ) versus shear rate (γ) for the ceramic suspensions: **a** S5–S8; **b** S11–S12

homogeneous ceramic suspension layer in the cell walls). The YSZ foams produced with the suspensions S6, S7, and S9, exhibited a brittle behavior, with the exception of the structures produced with the system S10. Therefore, this system (S10) was used to manufacture the YSZ foams.

For the samples produced with S10, the ppi and the anisotropy of the YSZ foams were established in two principal planes with height reference of 21 mm [2]. With a confidence level of 95% it was found that the YSZ foams fabricated with the 10 ppi and 20 ppi PUF presented pore densities of 12 ± 1 and 23 ± 1, respectively, and anisotropy close to the unit (≈ 1.03). The porosity of the ceramic structures was $93 \pm 3\%$ with a confidence level of 95%. The relative density is 0.07, which is relatively low compared with other foams produced for porous burners, e.g., SiC (0.13–0.14) and YZA (0.10–0.14) [14]. Additionally, a high mechanical strength is desirable for the ceramic foams, both for the building the system and for long operation times. A statistical analysis was performed with 95% of confidence, returned rupture stress as 95.62 ± 30.32 kPa of the YSZ foams.

Figure 4 shows SEM micrographs of the obtained YSZ foams. The micrographs revealed dense walls and open and interconnected cell structures (Fig. 4a). The grain boundaries in the YSZ foams tend to organize themselves forming angles of 120° between contiguous boundaries. Assuming that superficial tensions of each grain boundary have similar values, the microstructural analysis reveals a meta-stable state after sintering at 1600 °C (Fig. 4b). The macrostructure of the foams is homogeneous, without closed cells and apparently free from critical cracks that could result in catastrophic failure of the structure [15]. The micrograph of Fig. 4c shows a fractured surface of a strut, which contains no apparent defects that could promote its fracture.

In combustion processes in porous media the volume of fuel present in the reactor is measured with the equivalence ratio fuel/air (Φ). The radiation efficiency (Eq. 1) is defined as the amount of heat generated by the chemical reaction (Eq. 2) that is converted to the heat radiation of the structure (Eq. 3) [10].

$$\eta = Q_r/S_r. \tag{1}$$

$$S_r = m_c \Delta h_r. \tag{2}$$

$$Q_r = A_b \sigma \varepsilon \left(T_h^4 - T_o^4\right). \tag{3}$$

where T_h and T_o are the highest temperature and room temperature, respectively, Q_r is the heat emitted by radiation, S_r is the energy released by the reaction, Δh_r is the heat of the fuel reaction, m_c is the mass of flow fuel, and A_b is the effective area. In the calculations the effective emissivity of the medium was assumed to be equal to the unit ($\varepsilon = 1$).

Figure 5 shows the thermal behavior of the porous burners during operating conditions. The heat reached by the burner was relatively high (≈ 0.4 KW), taking into account only the contribution by radiation. High surface temperatures were recorded (1400 °C) without apparent damages of the porous structure in the macro-scale. Although the tests were performed at 1400 °C in steady state, peak temperatures of 1600 °C were registered before stabilization. Efficiencies higher than 19%, with a tendency toward stabilization with the increasing of the equivalence ratio were obtained. In comparison with the results of other researchers [16–18], the efficiencies are in the experimental range and even better at high fuel/air ratio.

Figure 6 shows the SEM micrographs of the YSZ foam after the burning test. As stated before, the foam maintained its structural integrity in the macro-scale (Fig. 6a). Figure 6b shows a hole at the surface of a strut that was originated from the gas release during polyurethane degradation. The grains grew up free from cracks maintaining the circular geometry of the hole. The fractured surface fracture of a strut is shown in Fig. 6c. No changes in the

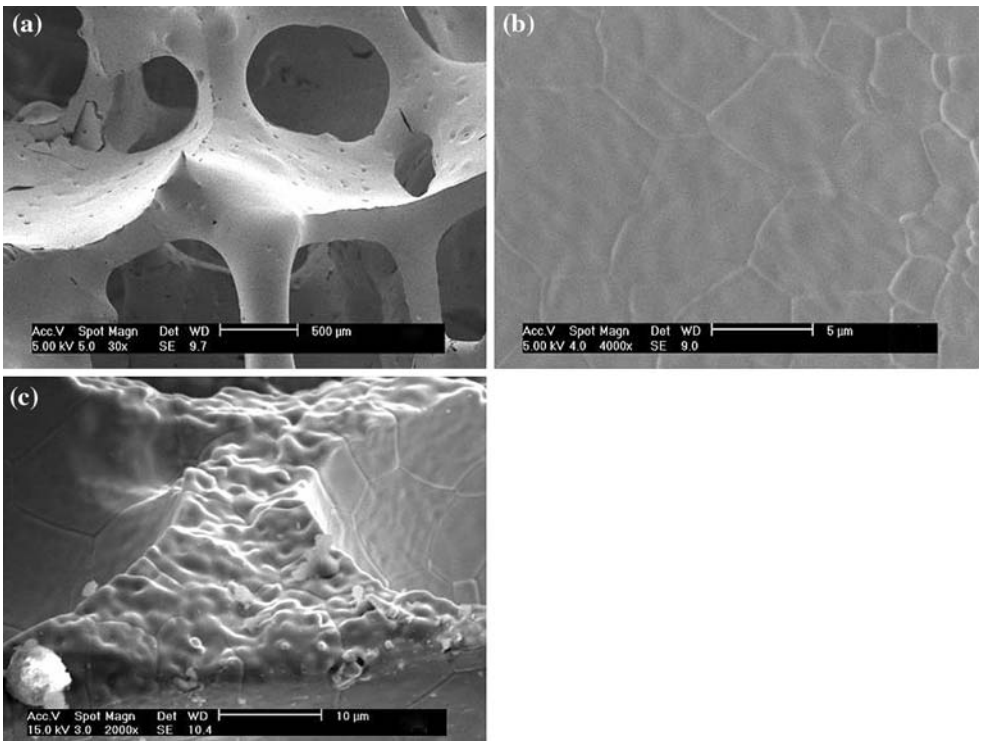

Fig. 4 SEM micrographs of the YSZ foams (23 ppi) sintered to 1600 °C. **a** Foam morphology; **b** Surface microstructure of a strut; **c** Microstructure of a fractured strut

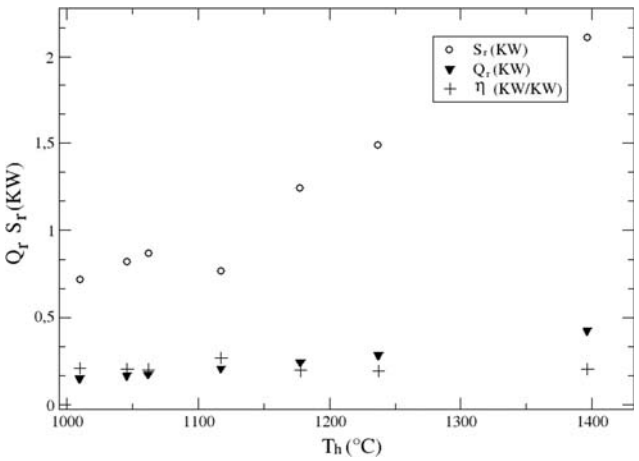

Fig. 5 Power released by the chemical reaction (S_r), radiation power (Q_r), and radiant efficiency (η) versus maximum burner temperature (T_h)

microstructure of the foams before (Fig. 4) and after the tests (Fig. 6) are visible, which confirms that YSZ foams resist at operation temperatures of 1400 °C. 8YSZ was chosen instead SiC in order to avoid the self-sustaining reaction of the last with air around 1400 °C. This reaction promotes a rapid increase in the temperature, melting the foam, and their ceramic isolation [10]. Moreover, although 8YSZ foams exhibit relatively low resistance to thermal shock compared to SiC, the propagation of a crack in these cellular structures causes failure of individual struts, but not a catastrophic damage [19, 20]. In fact, cellular structures with thinner struts or larger cells are more able to accommodate thermal strain by bending [11]. Additionally, lower relative densities give rise to lower thermal gradients along a single strut, which implies in a higher resistance of the bulk cellular structure to temperature variations.

Conclusions

Ceramic foams of YSZ with low relative density and interconnected open pores were successfully manufactured using the replication method. The appropriate impregnation was achieved using ceramic suspension with thixotropic and pseudoplastic behavior. These effects are attributed mainly to the additives Darvan C and PVA. Viscosity of the suspension can be adjusted by varying the amount of solids in suspension and grinding time. The S10 system exhibited appropriate rheological behavior compared to the other tested systems. At the temperature of 1600 °C a suitable sintering with meta-stable structure was reached. High mechanical strength under different work regimes, combined with high thermal efficiencies, revealed that the low relative density YSZ foams obtained are suitable for application as porous radiant burners at operating temperatures up to 1400 °C.

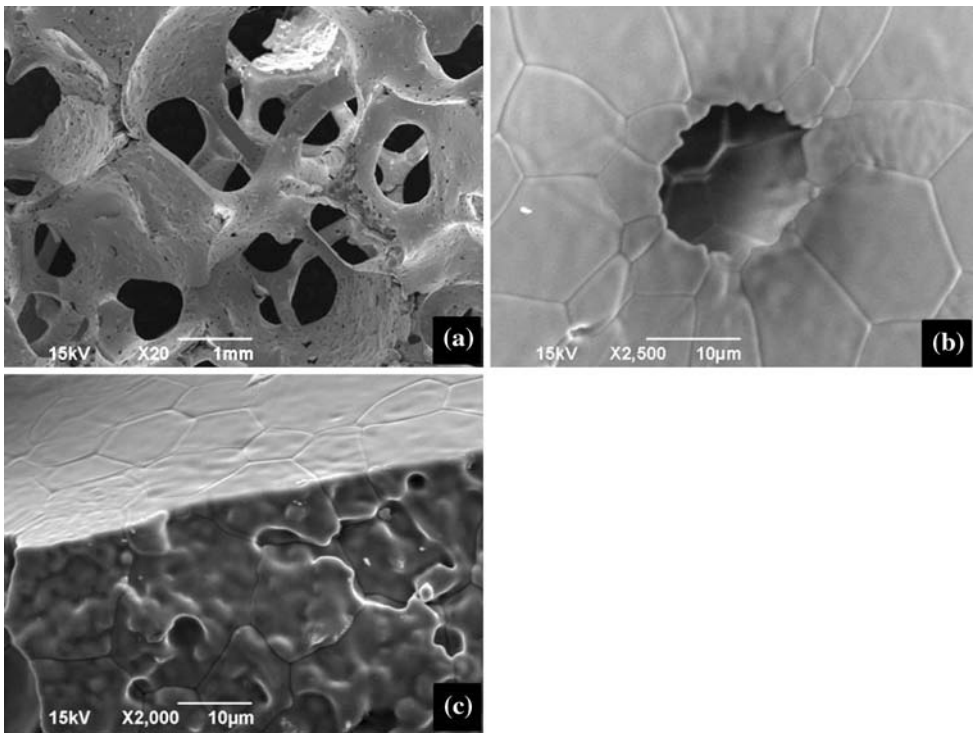

Fig. 6 SEM micrographs of a YSZ foam (23 ppi) after the burning test. **a** Foam morphology; **b** Surface microstructure of a strut; **c** Microstructure of a fractured strut

Acknowledgements The authors are grateful to Capes and CNPq/Brazil for funding this work. The authors are equally grateful to labCET (UFSC) for their collaboration with the porous burner's test.

References

1. Jugjai S, Rungsimuntuchart N (2002) Exp Therm Fluid Sci 26:581
2. Scheffler M, Colombo P (2005) Cellular ceramics structure: manufacturing properties and applications. Wiley-VCH, Weinheim
3. Bone W (1913) J Franklin Inst 2:101
4. Lucke C (1913) J Ind Eng Chem 5:801
5. Trimis D, Wawrzinek K, Hatzfeld O, Lucka K, Rutsche A, Haase F, Krüger K, Küchen C (2001) In: Proceedings of the 6th international conference on technologies and combustion for a clear environment, Porto, p 717
6. Hayashi TC, Malico I, Pereira JCF (2004) Comput Struct 82:1543
7. Mößbauer S, Pickenäcker O, Pickernäcker K, Trimis D (1999) In: Proceedings of the 5th international conference on technologies and combustion for a clean environment, Lisbon, p 519
8. Schwartzwalder K, Somers AV (1963) US Patent 3 090 094, May
9. Sousa E, Rambo CR, Hotza DD, Oliveira APN, Fey T, Greil P (2007) Mater Sci Eng A. doi:10.1016/j.msea.2007.05.098
10. Pereira F (2002) Medição de Características Térmicas e Estudo do Mecanismo de Estabilização de Chama em Queimadores Porosos Radiantes. Thesis (Master in Mechanical Engineering) UFSC, Brazil, 102 p
11. Gibson LJ, Asbhy MF (1997) Cellular solids: structure and properties. Cambridge University Press, London
12. Xinwen Z, Dongliang J, Shouhong T (2002) Mater Res Bull 37:541
13. Botella M (2005) Reología de Suspensiones Cerámicas. Consejo Superior de Investigaciones Científicas (CSIC), Madrid
14. Vedula VR, Green DJ, Hellman JR (1999) J Am Ceram Soc 82(3):649
15. Elverum PJ, Ellzey JL, Kovar D (2005) J Mater Sci 40:155. doi:10.1007/s10853-005-5701-6
16. Khannan R, Goel R, Ellzey JL (1994) Combust Sci Technol 99:133
17. Pereira FM, Catapan RC, Oliveira AAM (2005) Development of a radiant porous burner with a combined thermal and fluidynamic mechanism of flame stabilization. In: 18th international congress of mechanical engineering, Ouro Preto, Brazil, 2005
18. Barra AJ, Ellzey JL (2004) Combust Flame 137:230
19. Orenstein RM, Green DJ (1992) J Am Ceram Soc 75(7):1899
20. Brezny R, Green DJ (1989) J Am Ceram Soc 72(7):1145